A seasonal trend of single scattering albedo in southern African biomass-burning particles: Implications for satellite products and estimates of emissions for the world's largest biomass-burning source

T. F. Eck,[1,2] B. N. Holben,[2] J. S. Reid,[3] M. M. Mukelabai,[4] S. J. Piketh,[5] O. Torres,[2] H. T. Jethva,[1,2] E. J. Hyer,[3] D. E. Ward,[6] O. Dubovik,[7] A. Sinyuk,[2,8] J. S. Schafer,[2,8] D. M. Giles,[2,8] M. Sorokin,[2,8] A. Smirnov,[2,8] and I. Slutsker[2,8]

Received 19 February 2013; revised 10 May 2013; accepted 16 May 2013; published 19 June 2013.

[1] As a representative site of the southern African biomass-burning region, sun-sky data from the 15 year Aerosol Robotic Network (AERONET) deployment at Mongu, Zambia, was analyzed. For the biomass-burning season months (July–November), we investigate seasonal trends in aerosol single scattering albedo (SSA), aerosol size distributions, and refractive indices from almucantar sky scan retrievals. The monthly mean single scattering albedo at 440 nm in Mongu was found to increase significantly from ~0.84 in July to ~0.93 in November (from 0.78 to 0.90 at 675 nm in these same months). There was no significant change in particle size, in either the dominant accumulation or secondary coarse modes during these months, nor any significant trend in the Ångström exponent (440–870 nm; $r^2 = 0.02$). A significant downward seasonal trend in imaginary refractive index ($r^2 = 0.43$) suggests a trend of decreasing black carbon content in the aerosol composition as the burning season progresses. Similarly, burning season SSA retrievals for the Etosha Pan, Namibia AERONET site also show very similar increasing single scattering albedo values and decreasing imaginary refractive index as the season progresses. Furthermore, retrievals of SSA at 388 nm from the Ozone Monitoring Instrument satellite sensor show similar seasonal trends as observed by AERONET and suggest that this seasonal shift is widespread throughout much of southern Africa. A seasonal shift in the satellite retrieval bias of aerosol optical depth from the Moderate Resolution Imaging Spectroradiometer collection 5 dark target algorithm is consistent with this seasonal SSA trend since the algorithm assumes a constant value of SSA. Multi-angle Imaging Spectroradiometer, however, appears less sensitive to the absorption-induced bias.

Citation: Eck, T. F., et al. (2013), A seasonal trend of single scattering albedo in southern African biomass-burning particles: Implications for satellite products and estimates of emissions for the world's largest biomass-burning source, *J. Geophys. Res. Atmos.*, *118*, 6414–6432, doi:10.1002/jgrd.50500.

1. Introduction

[2] Southern Africa has consistently been identified as the world's largest single source of biomass-burning emissions [*Crutzen and Andreae*, 1990; *Giglio et al.*, 2003a, 2006, 2010; *Reid et al.*, 2009; *van der Werf et al.*, 2010], and therefore, this region is important to any global budget of greenhouse gas, aerosol, or black carbon emissions. A topic of critical importance to aerosol research in this region is particle light absorption. Aerosol spectral absorption has been measured at numerous sites globally in a consistent manner by sun-sky radiometers in the Aerosol Robotic Network (AERONET) [*Holben et al.*, 1998; *Dubovik et al.*, 2002] using common calibration and data processing procedures. Among the most absorbing aerosol particles (lowest single scattering albedo (SSA)) measured at any AERONET sites are those occurring during the biomass-burning season in Zambia in the southern Africa savanna-burning region [*Dubovik et al.*, 2002; *Giles et al.*, 2012]. This results from the relatively high fraction of flaming versus smoldering combustion that occurs during grass burning in the savanna environment, compared to the larger fraction of smoldering combustion of woody fuels in some other environments, as

[1]Universities Space Research Association, Columbia, Maryland, USA.
[2]NASA Goddard Space Flight Center, Greenbelt, Maryland, USA.
[3]Naval Research Laboratory, Monterey, California, USA.
[4]Zambian Meteorological Department, Lusaka, Zambia.
[5]School of Geo- and Spatial Sciences, North-West University, Potchefstroom, South Africa.
[6]Enviropyronics, White Salmon, Washington, USA.
[7]Universite de Lille, Villeneuve d'Ascq, France.
[8]Sigma Space Corporation, Lanham, Maryland, USA.

Corresponding author: T. F. Eck, NASA Goddard Space Flight Center, Code 618, Greenbelt, MD 20771, USA. (thomas.f.eck@nasa.gov)

2169-897X/13/10.1002/jgrd.50500

had been measured in situ during controlled burns by *Ward et al.* [1992, 1996].

[3] From a climate point of view, aerosol absorption is a key parameter affecting the aerosol direct radiative forcing at the top of the atmosphere, solar radiation incident at the surface, and radiative heating of the aerosol layer. All of these impacts have significant consequences on atmospheric stability and perhaps clouds through the semidirect effect [*Pilinis et al.*, 1995; *IPCC*, 2007]. Seasonal variation of spectral SSA has been observed to occur at some AERONET sites (Kanpur, India; Beijing, China; and Ilorin, Nigeria) where there are varying mixtures of fine- and coarse-mode aerosol particles [*Eck et al.*, 2010], with the relative abundance of the two distinct aerosol types (i.e., desert dust and pollution or smoke) driving much of the annual variation. Additionally, a multiyear trend in aerosol absorption was detected at Beijing with AERONET retrieved SSA by *Lyapustin et al.* [2011], made possible by the very high aerosol optical depths (AODs) at that site, since the sensitivity to absorption increases significantly as AOD increases. These results indicate that perhaps using a fixed SSA value may lead to uncertainty in forcing calculations at some locations.

[4] For southern Africa, with its significant smoke particle sources, high AOD, low particle SSA, and sometimes complex coastal stratocumulus cloud patterns, we would expect a significant impact of aerosol particles on the atmosphere. However, a wide variety of assumptions can be made regarding particle properties such as SSA to help parameterize absorption. For example, recently, *Chand et al.* [2009], *Sakaeda et al.* [2011], and *Wilcox* [2012] have estimated the direct and semidirect radiative forcing of biomass-burning aerosols over stratocumulus clouds off of the western tropical Atlantic coast of Africa (equator to 20°S in *Wilcox* [2012]; 10°N–30°S in *Sakaeda et al.* [2011]; 7.5°S–22.5°S in *Chand et al.* [2009]). The columnar weighted SSA computed by *Sakaeda et al.* [2011] ranged from ~0.97 to 0.86. This wide range of computed SSA values is partly the result of a variability of aerosol species other than carbonaceous species included in their model. On the other hand, *Wilcox* [2012] assumed a constant SSA value of 0.89 at 550 nm for the months of July–September, while Chand assumed a constant value of 0.85 in the midvisible for July–October. Diversity in assumed SSA values such as reported here translates to community-wide uncertainty in the effects of aerosol particles in the regional climate, particularly for cases of aerosol particles over clouds where the impact of aerosol absorption is enhanced.

[5] A second area of importance of aerosol absorption and SSA is in the sensitivities of some satellite AOD retrievals. Particle absorption, particularly in multiple scattering environments (say AOD > 0.5), plays an increasingly important role in top of atmosphere (TOA) radiances used by satellites to infer AOD. Some satellite algorithms such as for the Moderate Resolution Imaging Spectroradiometer (MODIS) collection 5 (C5) over land algorithm assume regional SSAs in their calculations [*Levy et al.*, 2007a, 2007b], while products such as from the Multi-angle Imaging Spectroradiometer (MISR) algorithm [*Kahn et al.*, 2010] try to account for the impact of varying absorption on retrieved AOD. *Robles-Gonzalez and de Leeuw* [2008] presented a satellite retrieval algorithm utilizing ATSR-2 data that attempted to account for changes in aerosol absorption. This algorithm was applied to data over southern Africa; however, they concluded that aerosol properties were not accurately retrieved for strongly absorbing aerosols resulting from biomass burning. More recently, *Holzer-Popp et al.* [2013] discuss several satellite retrieval algorithms developed for application to European Earth observation satellite sensor data, some of which account for variation in aerosol absorption properties.

[6] With its high and consistent aerosol signal, the Mongu site in southern Africa has been a widely utilized location to verify satellite aerosol products. Indeed, it is the only long-term AERONET site with proximity to the south African smoke plume, and many AOD verification studies are highly dependent on that particular site. For example, *Ichoku et al.* [2003] found that the previously assumed regional SSA value for southern Africa of 0.90 in early MODIS retrievals for this region resulted in significant underestimates of AOD from the MODIS sensor, especially at high AOD, while an assumed value of 0.87 at 470 nm would have yielded much more accurate values. Even after iteration, the current MODIS C5 still retains a substantial regional low bias, attributed to error in absorption assumptions [*Hyer et al.*, 2011]. *Kahn et al.* [2010] also included performance metrics of MISR to the southern African biomass-burning plume using data from Mongu as a representative site.

[7] In early analysis of the Mongu AERONET site, it was noticed that the southern African smoke plume single scattering albedo exhibits a significant and robust seasonal cycle. This led to questions on the cycle's implications for both smoke radiative forcing and on satellite AOD retrievals in the world's largest smoke source. By extension, there are then further questions regarding attempts to invert smoke emissions from satellite data. In this paper, we will focus on the seasonal variation of aerosol absorption at AERONET sites in the southern Africa region during the biomass-burning season of July to November [*Swap et al.*, 2003]. In the first part, we describe the nature of seasonal variability in smoke single scattering albedo at the Mongu site. In the second part, we examine the implications of variability in single scattering albedo in satellite aerosol products, such as in aforementioned MODIS and MISR retrievals of AOD. In addition, we examine recent algorithms that have been developed to retrieve aerosol SSA from satellite-measured UV radiances [*Torres et al.*, 2005; *Jethva and Torres*, 2011]. We conclude with a discussion on the implications of our findings on aerosol radiative forcing and inverse modeling estimates of the smoke source magnitude.

2. Instrumentation, Study Sites, Data, and Techniques

2.1. Study Region and AERONET Sites

[8] A map showing the locations of the AERONET sun-sky radiometers utilized in this study is shown in Figure 1a. The principal AERONET site analyzed in this study is the Mongu, Zambia site (15°15′S; 23°09′E) located in western Zambia and selected to characterize the biomass-burning aerosols in this region of extensive savanna burning (note numerous fire counts in Figure 1b). The data set at Mongu is one of the longest and most complete sets of aerosol optical properties measurements made at any site in the AERONET network, beginning in June 1995 and continuing

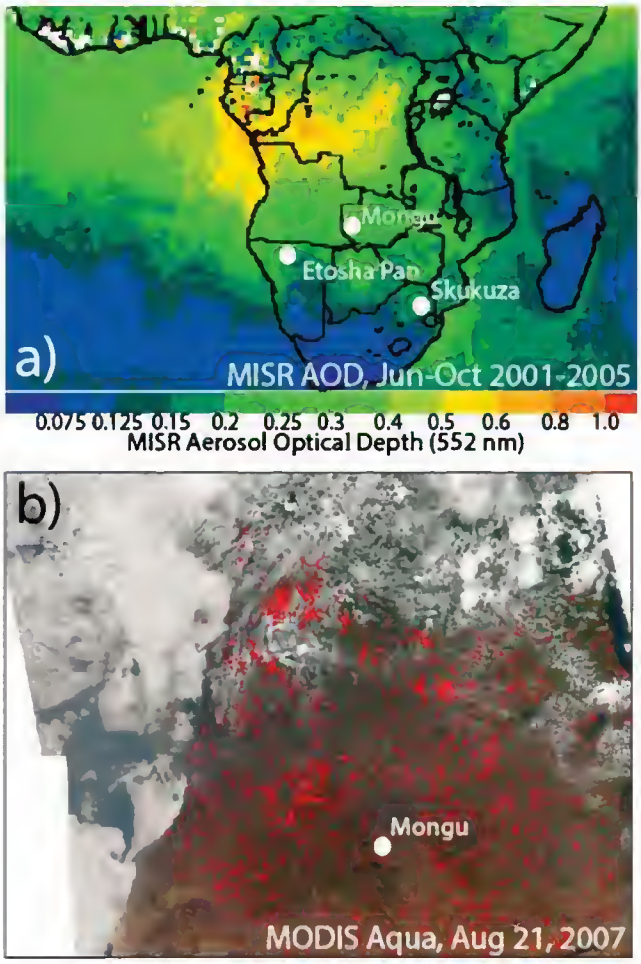

Figure 1. (a) Average midvisible AOD retrieved from MISR for the primary southern Africa burning season months of June to October for the years 2001 to 2005. Also shown are the AERONET sites discussed in this paper located within this biomass-burning region. (b) A single-day MODIS image from 21 August 2007 showing the fire counts in red and the location of the Mongu AERONET site.

through 2009. However, the retrievals of SSA from Mongu were not available from 2005 to 2009 due to problems with either the temperature sensor (needed in order to correct the 1020 nm data) and/or obstructions in the collimator that measures sky radiances. Other AERONET sites which were analyzed in this study were located in Etosha Pan National Park (19°10′S; 15°54′E), Namibia and Skukuza (25°59.5′S; 31°35′E; in Kruger National Park), South Africa. The time period of the analysis, which is July to early November, coincides with the biomass burning associated with agricultural practices and land management and thus the highest levels of AOD from biomass burning [*Scholes et al.*, 1996]. Subsidence from anticyclonic circulation is a dominant meteorological feature during much of the biomass-burning season in this region with four stable vertical layers identified in the troposphere [*Garstang et al.*, 1996; *Anderson et al.*, 1996]. Altitudinal layering of aerosols associated with temperature inversions was observed with a micropulse lidar at a site in South Africa during SAFARI 2000 [*Campbell et al.*, 2003]. This atmospheric stability often results in cloudless or nearly cloudless sky conditions for extended periods over land for much of the biomass-burning season.

2.2. AERONET Instrumentation

[9] The Cimel Electronique CE-318 sun-sky radiometer measurements reported in this paper were made with instruments that are a part of the Aerosol Robotic Network (AERONET) global network. These instruments are described in detail in *Holben et al.* [1998]; however, a brief description will be given here. The automatic tracking Sun and sky scanning radiometers made direct Sun measurements with a 1.2° full field of view every 15 min at 340, 380, 440, 500, 675, 870, 940, and 1020 nm (nominal wavelengths). The direct Sun measurements take ~8 s to scan all eight wavelengths, with a motor-driven filter wheel positioning each filter in front of the detector. These solar extinction measurements are then used to compute aerosol optical depth (AOD) at each wavelength except for the 940 nm channel, which is used to retrieve total columnar (or precipitable) water vapor in centimeters. The filters utilized in these instruments were ion-assisted deposition interference filters with band pass (full width at half maximum) of 10 nm, except for the 340 and 380 nm channels at 2 nm band pass. The estimated uncertainty in measured AOD, due primarily to calibration uncertainty, is ~0.010–0.021 for field instruments (which is spectrally dependent with the higher errors in the UV) [*Eck et al.*, 1999]. *Schmid et al.* [1999] compared AOD values derived from four different solar radiometers (including an AERONET sun-sky radiometer) operating simultaneously together in a field experiment and found that the AOD values from 380 to 1020 nm agreed to within 0.015 (root-mean-square; RMS), which is similar to our estimated level of uncertainty in AOD measurement for field instruments. The spectral aerosol optical depth data (all data are AERONET version 2 level 2) have been screened for clouds following the methodology of *Smirnov et al.* [2000], which relies on the greater temporal variance of cloud optical depth versus aerosol optical depth. The sky radiances measured by the sun/sky radiometers are calibrated versus the 2 m integrating sphere at the NASA Goddard Space Flight Center, to an absolute accuracy of ~5% or better.

2.3. Inversion Methodology

[10] The Cimel sky radiance measurements in the almucantar geometry (fixed elevation angle equal to solar elevation and a full 360° azimuthal sweep) at 440, 675, 870, and 1020 nm (nominal wavelengths) in conjunction with the direct sun-measured AOD at these same wavelengths were used to retrieve optical equivalent aerosol size distributions and refractive indices. Using this microphysical information, the spectral dependence of SSA is calculated. The algorithm of *Dubovik and King* [2000] with enhancements detailed in *Dubovik et al.* [2006] was utilized in these retrievals, known as Version 2 AERONET retrievals. Level 2 quality-assured retrievals [*Holben et al.*, 2006] are presented in this paper. The Version 2 AERONET algorithm determines the percentage of spherical (versus spheroidal shape) particles required to give the best fit to the measured spectral sky radiance angular distribution. Further details on the Version 2 algorithm and the improved specification of

surface bidirectional reflectance can be found in *Dubovik et al.* [2006] and *Eck et al.* [2008].

[11] Almucantar sky radiance measurements were made at optical air masses of 4, 3, 2, and 1.7 in the morning and afternoon, and once per hour in between. In order to ensure sky radiance data over a wide range of scattering angles, only almucantar scans at solar zenith angles (SZA) greater than 50° are analyzed and presented here (the maximum SZA is ~76°). To eliminate cloud contamination from the almucantar directional sky radiance data, we require the radiances to be symmetrical on both sides of the Sun at equal scattering angles [*Holben et al.*, 2006]. The stable performance of the inversion algorithm was illustrated in sensitivity studies performed by *Dubovik et al.* [2000] where the perturbations of the inversion resulting from random errors, possible instrument offsets, and known uncertainties in the atmospheric radiation model were analyzed. Their work employed retrieval tests using known size distributions to demonstrate successful retrievals of mode radii and the relative magnitude of modes for various types of bimodal size distributions such as those dominated by a submicron accumulation mode or distributions dominated by supermicron coarse mode aerosols. To ensure sufficient sensitivity to aerosol absorption, only almucantar scans where AOD (440 nm) > 0.4 [*Dubovik et al.*, 2000] were analyzed for the investigation of the characteristics of spectral refractive indices and single scattering albedo. Although very few direct comparisons of size distribution between in situ and AERONET retrievals have been made, there are several aerosol types in specific regions that have been or can be compared. For example, *Reid et al.* [2005a] present a table where the volume median radius of smoke from various major biomass-burning regions (South America, southern Africa, North America (boreal, temperate)) are compared. For all three of these regions, the volume median diameters of the in situ versus the AERONET retrievals are often within ~0.01 μm of each other. Additionally, for fine-mode biomass-burning aerosols in southern Africa (including Zambia), *Leahy et al.* [2007] found a mean discrepancy in 550 nm SSA between in situ measurements and AERONET retrievals of −0.01 for five coincident flights over AERONET sites, thus indicating excellent agreement.

2.4. MODIS and MISR Satellite Retrievals of AOD

[12] In this study, we examine the potential for SSA induced bias in satellite AOD retrievals from three primary datasets. First, the over land MODIS data C5 products of *Levy et al.* [2007a] which were co-located with AERONET AOD data at the Mongu site within ±30 min of overpass. These retrievals vary in size from 10 × 10 km at nadir, to ~40 × 20 km at the swath edge. *Hyer et al.* [2011] compared MODIS retrieved AOD to AERONET retrievals from the Mongu site for 2005–2008 and found r^2 of 0.61/0.56 and slope biases of 0.83/0.88 for Terra and Aqua MODIS, respectively. In general for southern Africa, *Hyer et al.* [2011] found that prognostic RMS errors were on the order of the greater of 0.06 or $0.00 + 0.28\ \mathrm{AOD}_T$ for Terra and 0.07 or $-0.02 + 0.39 * \mathrm{AOD}_A$ for Aqua where the AOD is taken as the retrieved AOD. Much of this RMS error can be attributed to the slope biases. In the current paper, we also examined MISR v22 retrievals [*Diner et al.*, 2010] in like manner to the operational MODIS C5. Retrieval size is 21 × 21 km throughout the swath. *Kahn et al.* [2010] examined MISR performance at the Mongu site, finding excellent correlation ($r^2 = 0.9$) but a slight low bias (slope of 0.84). To our knowledge, no RMS errors have been formulated for the site, outside of what we will present later in this paper. Intercomparison of MODIS and MISR data by *Shi et al.* [2011] showed reasonable regression coefficients for collocated retrievals (r^2 range from 0.7 to 0.85) but with MODIS having 20% higher values in slope. This result is somewhat at odds with AERONET-based comparisons.

[13] In addition to the standard operational MODIS and MISR products, we also examined the level 3 operational data assimilation grade MODIS product [*Hyer et al.*, 2011] used by the US Navy [*Zhang et al.*, 2008]. In this product, data are screened for a number of known artifacts, regression corrections are made for region-wide biases, and a final 1 × 1° aggregated product is generated. Estimated prognostic RMS errors for this product are the greater of 0.05 or $0.03 + 0.19\ \mathrm{AOD}_T$ for Terra and 0.05 or $-0.01 + 0.21 * \mathrm{AOD}_A$. Much of this improvement is due to the implementation of a regional slope correction.

2.5. OMI Satellite Retrievals of SSA

[14] The Ozone Monitoring Instrument (OMI) on the Aqua satellite is a high-resolution spectrograph in operation since September 2004 [*Levelt et al.*, 2006]. OMI observations at 354 nm and 388 nm are used in an inversion algorithm (OMAERUV) to retrieve aerosol single scattering albedo [*Torres et al.*, 2007]. The physical basis for detecting and quantifying aerosol absorption in the near UV is the interaction between molecular scattering and particle absorption that generates a unique signal clearly associated with aerosol absorption [*Torres et al.*, 1998]. This radiative transfer interaction is the basis of the Absorbing Aerosol Index, a qualitative indicator of aerosol absorption, developed originally from TOMS observations [*Hsu et al.*, 1996; *Herman et al.*, 1997], and produced routinely since then from observations by sensors with near-UV observing capability. Quantitative information on aerosol absorption can be derived by an inversion procedure. The OMAERUV retrieval technique uses precalculated radiances at 354 and 388 nm to simultaneously retrieve both aerosol optical depth and single scattering albedo. A priori information on particle size distribution and aerosol layer height is required. Retrieval algorithm details are given in *Torres et al.* [2007], and recent upgrades are discussed by *Jethva and Torres* [2011] and *Torres et al.* [2012].

3. Results

3.1. Seasonal Variation of Aerosol Absorption—AERONET Data

[15] Multiyear measurements made by the Cimel sun-sky radiometer at the AERONET site in Mongu, Zambia provide the most complete data set to investigate the seasonality of aerosol optical depth and absorption in the southern Africa biomass-burning region. In Figure 2, we present the monthly averages of Level 2 direct sun-measured 500 nm AOD at Mongu from measurements made from 1995 to 2009, similar to that shown in *Queface et al.* [2011]. Monthly means were computed from daily means, with a minimum of 9 days per month used as a threshold for good sampling, resulting in

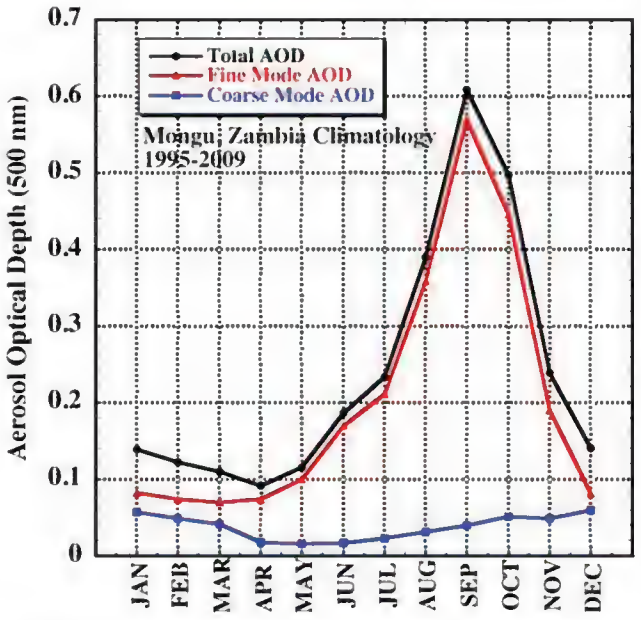

Figure 2. Monthly mean AOD at 500 nm at the Mongu, Zambia AERONET site from 1995 to 2009. A threshold of 9 days minimum per month was required to ensure adequate sampling, resulting in 8 to 13 years of data being averaged for each month. The fine- and coarse-mode AODs were computed using the Spectral Deconvolution Algorithm (SDA).

8 to 13 years of data being averaged for each month. The biomass-burning season in Mongu begins in June with elevated AOD and ends in November. Also shown in Figure 2 are the fine- and coarse-mode AOD values that are computed from the Spectral Deconvolution Algorithm (SDA) described in *O'Neill et al.* [2001, 2003] based on the measured AOD spectra from 380 to 870 nm and the assumption of a bimodal size distribution. The SDA retrievals of fine mode fraction (FMF) of AOD at 500 nm are ~0.03 to 0.05 lower on average than almucantar-retrieved FMF [*Eck et al.*, 2010], likely due in part to the small-sized particle "wing" of the coarse mode attributed to coarse-mode AOD in the SDA, while this wing is included in the fine mode of the Dubovik algorithm since a particle radius cutoff is selected to define the two modes [*O'Neill et al.*, 2003]. Another possible reason for the bias could be that the SDA retrieval does not explicitly account for effects of variation in the refractive index, which is a source of SDA retrieval error. It can be seen in Figure 2 that fine-mode aerosol particles dominate the total AOD during the biomass-burning season, while coarse-mode AOD is elevated in the rainy season, likely due to some cloud contamination in those months [*Eck et al.*, 2003].

[16] The data shown in Figure 3 are daily averages of single scattering albedo for years with significant numbers of almucantar retrievals at the Mongu site, 1997 to 2005, excluding 2000. The year 2000 data were excluded due to a problem with the sky radiance calibration for that instrument in that year [*Eck et al.*, 2003]. The SSA retrievals at 440 nm are shown only for observations where AOD at 440 nm exceeded 0.4, thus ensuring sufficient aerosol loading to limit SSA uncertainty at ~0.03 or less. In Figure 3a, data are shown from May to November, and it is noted that from late May to early June, the SSA values show a relatively large degree of variability with some higher values than measured in July. The reason for this large variability in the May–June preseason is not well known. It may possibly be caused in part by smoke from burning to the north of Zambia, some of which is more densely forested. Clearly, the majority of the data with moderate to high AOD occur from July to October plus a few in November (a total of 300 days of data), as this is the primary biomass-burning season in the region that is predominantly savanna and woodland [*Cooke et al.*, 1996]. Therefore, we will focus on this time period for further analysis of the Mongu data. Figure 3b shows the daily average SSA data time series for the months of July–November, and there is clearly a linear trend of increasing SSA as the burning season progresses, with a linear fit explaining 49% of the variance. It is noted that we found no trend of SSA as a function of AOD magnitude ($r^2 = 0.02$). What we did

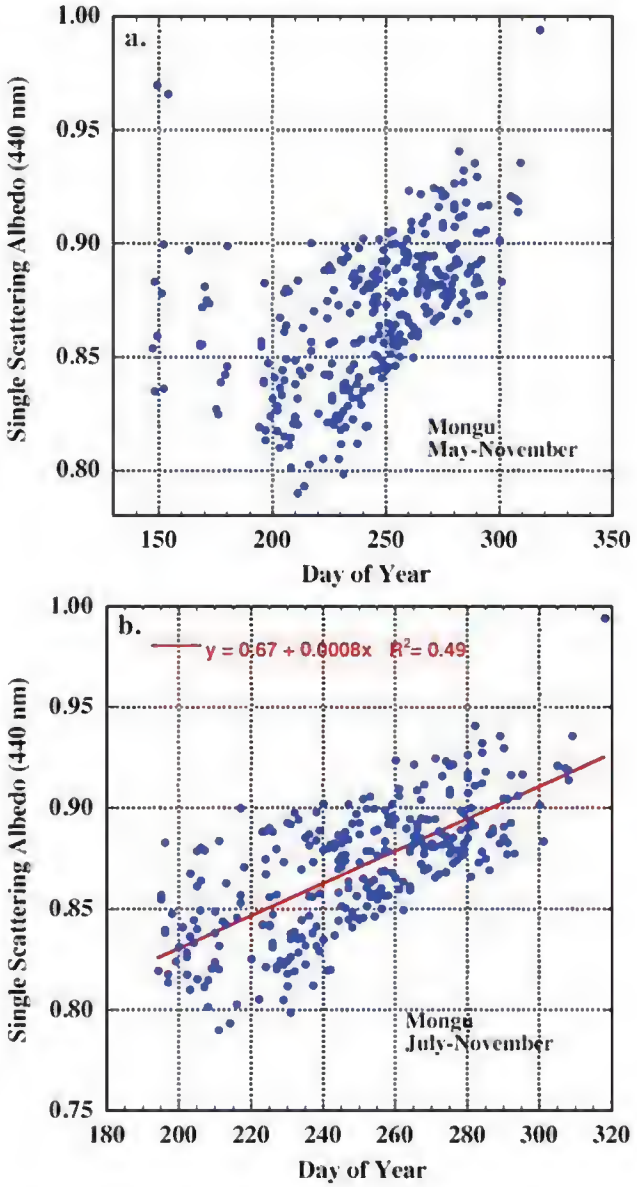

Figure 3. Time series of single scattering albedo (440 nm) at Mongu, Zambia for cases where AOD (440 nm) > 0.4 from (a) May to November and from (b) July to November, the main biomass-burning season.

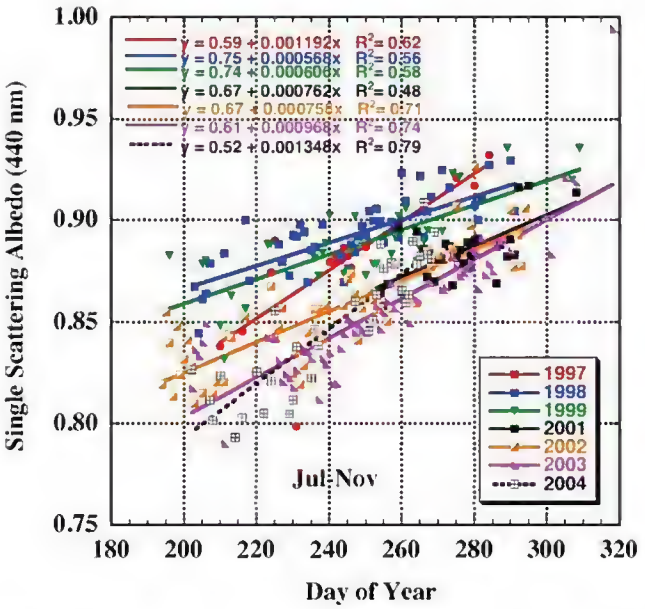

Figure 4. Similar to Figure 3b, the burning season time series of SSA (440 nm) for Mongu, but with linear regression analysis made on each year separately.

find, however, was that there is an interannual shift in the overall SSA magnitude. This is demonstrated in Figure 4 where the data for the individual years are analyzed separately. It is hence noted that part of the scatter in Figure 3 is due to variation in SSA magnitudes between years, with higher values in 1997–1999. The data for all 7 years however show a similar increase in SSA through the entire burning season with linear regression fits explaining from 48% to 79% of the variance in individual years. The year 2005 was excluded in this figure since nearly all data from August and September 2005 were missing due to logistical problems. The reason for the higher SSA values in 1997–1999 is unknown, but may possibly be due to interannual differences in biomass fuel types (woody versus grasses) burned in different proportions, but may also be due to biases in the Cimel sky radiance calibrations from year to year. The accuracy of the direct sun AOD measurement is highly accurate (~0.01 in visible and near infrared) [*Eck et al.*, 1999] but the sky radiance calibration uncertainty is larger at less than 5% [*Holben et al.* 1998]. The magnitude of the sky radiances will directly affect the retrievals of SSA; therefore, the early year data may possibly be biased high due only to calibration uncertainty. However, regardless of this interannual variability, the data from all individual years show a similar strongly increasing SSA, meaning increasingly weaker absorption, from the beginning to the end of the burning season.

[17] The monthly mean spectral variation of SSA from 440 nm to 1020 nm (all four of the retrieved wavelengths) from the same days as shown in Figure 3b is shown in Figure 5 averaged by month. Although the mean AOD and fine-mode AOD in November are similar to the July monthly mean [*Eck et al.*, 2003; *Queface et al.*, 2011], only six good retrievals of SSA were available in November in all these years of monitoring; this is due to the rapid increase in cloud cover accompanying the start of the rainy season (the dry season months of April–October contribute <10% of the annual mean rainfall amount). A direct sun measurement of AOD can be made in a gap between clouds while the SSA retrieval requires a mostly cloud-free sky radiance scan over a full azimuthal sweep at constant elevation angle equal to the sun elevation (from 15° to 40° elevation angle for a Level 2 almucantar scan). While significant smoke is present in November, the sparseness of the SSA data for this month results in this analysis being more uncertain. We will therefore concentrate on the months of July to October in the following discussion of Figure 5. The SSA at 440 nm in October is 0.058 higher than in July, and the October–July mean SSA differences for 675, 870, and 1020 nm are 0.076, 0.086, and 0.091, respectively. These are large seasonal changes in SSA that may have significant impacts on the retrieval of AOD from satellite using algorithms that require a priori assumption of SSA [*Ichoku et al.*, 2003], and also result in significant changes in aerosol direct and semidirect radiative forcings. It is noted that the climatological average SSA values for African savanna in Zambia (mostly data from Mongu) given by *Dubovik et al.* [2002] from pre-Version 1 AERONET data are within 0.01 or less at all wavelengths of the September monthly mean shown in Figure 4. The updated Version 2 database SSA climatology given by *Giles et al.* [2012] for Mongu (based on the entire season) is also within 0.01 of the September average shown in Figure 5, except for 1020 nm which is 0.02 higher than *Giles et al.* (2012). This similarity in climatological biomass-burning season average to the September monthly mean occurs since September has the most retrievals of any month and since lower SSA values are retrieved in July and August and higher SSA in October and November.

[18] The spectral variation of SSA can further be characterized by the variation in the aerosol absorption Ångström exponent. The absorption Ångström exponent (AAE) is computed from spectral absorption optical depths (AAODs)

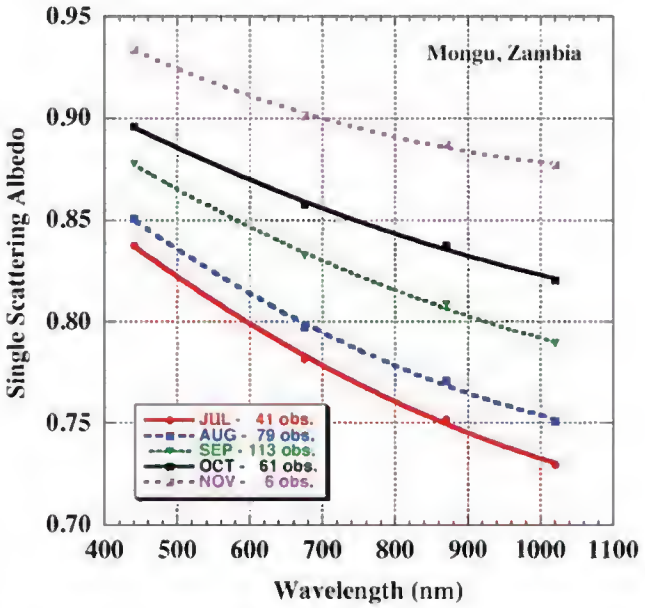

Figure 5. Monthly mean values of spectral SSA for Mongu Zambia from 1997 to 2005 for the burning season months, for all four retrievals wavelengths (440, 675, 870, and 1020 nm).

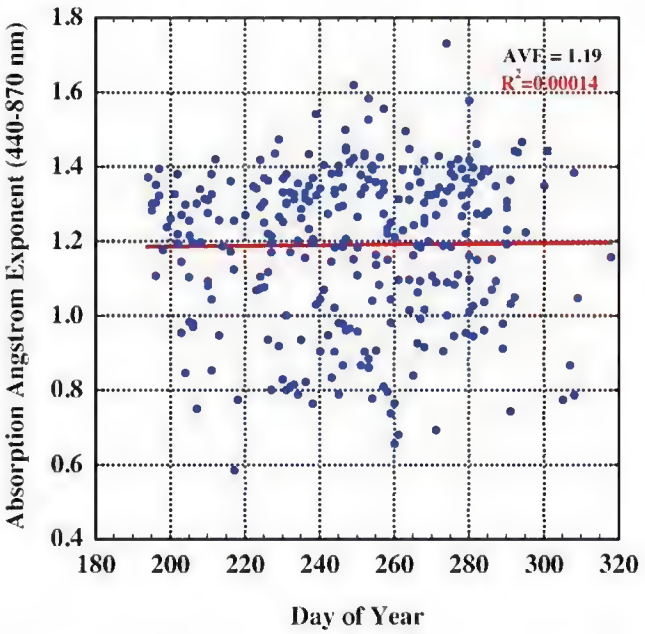

Figure 6. The time series of daily average absorption Ångström exponents (440–870 nm) for the biomass-burning season at Mongu Zambia, showing a lack of any seasonal trend.

which are in turn computed from spectral total extinction AOD and SSA by

$$\mathrm{AAOD} = \mathrm{AOD}\,(1 - \mathrm{SSA}) \tag{1}$$

[19] The negative of the mean fitted slope of the AAOD with wavelength in logarithmic coordinates defines the AAE. Daily mean values of AAE for Mongu from July to November are shown in Figure 6 for the same years as shown in Figure 3. The majority of the daily mean values of AAE ranged from ~0.80 to 1.5 with an overall biomass-burning season mean of 1.19. Theoretically, fine-mode aerosol with absorption determined exclusively by black carbon (BC) would have AAE equal to 1.0, since BC is expected to have a spectrally constant imaginary refractive index (k) [*Bergstrom et al.*, 2002; *Bergstrom et al.*, 2007]. In fact, the retrievals of imaginary refractive index (k) for this Mongu data do show relatively small wavelength dependence, as seen in the spectral monthly means in Figure 7. Therefore, this seasonal mean value of AAE of ~1.20 at Mongu and small spectral variation of imaginary refractive index both suggest that BC is the dominant absorber in the visible and near-infrared wavelengths for this biomass-burning aerosol, which is consistent with in situ measurements [*Ward et al.*, 1996; *Reid and Hobbs*, 1998]. There is also a lack of any seasonal trend in daily average AAE at Mongu (Figure 6; $r^2 = 0.0001$), therefore implying that BC is the dominant absorbing aerosol component throughout the entire biomass-burning season. For smoke produced by combustion of various biomass fuels, measured in situ under controlled laboratory conditions, *Lewis et al.* [2008] found AAE as high as 2.5 (532 to 870 nm) at high SSA (near unity) while AAE values approached 1.0 for SSA < 0.8 at 532 nm. The measured organic carbon to total carbon ratio was highest for the smoke with the highest AAE and SSA and lowest for the lowest SSA values measured.

[20] To further investigate the reasons for the trend in aerosol single scattering albedo throughout the biomass-burning season, we examine data on both the retrieved aerosol size and the complex refractive indices. In Figure 8a we show the daily averages of Ångström exponent (440–870 nm) computed using direct sun-measured AOD at 440, 500, 675, and 870 nm from linear regression, for July to November (associated with the retrieval dates and times in Figure 3b). The Ångström exponent computed from a wide wavelength range has been shown to be a general indicator of particle size and fine/coarse-mode fraction [*Eck et al.*, 1999; *Eck et al.*, 2010]. The values of $a_{440\ 870}$ range primarily from ~1.7 to ~2.0 with a mean of 1.85 which is typical of fine-mode (submicron radius) dominated aerosol from biomass-burning regions [*Holben et al.*, 2001; *Eck et al.* 2003; *Schafer et al.*, 2008]. Additionally, the lack of any seasonal trend ($r^2 = 0.02$) in $a_{440\ 870}$ suggests that the particle size and fine-mode fraction did not change significantly from July to November. The short wavelength range Ångström exponent (380–500 nm) is much more sensitive to variation in fine-mode particle size [*Reid et al.*, 1999; *Eck et al.*, 2001], and this also exhibited no significant seasonal trend ($r^2 = 0.06$; mean = 1.52; not shown). It is noted that the SDA fine-coarse mode AOD shown in Figure 2 would suggest a decrease in Ångström exponent at the end of the burning season in October and especially in November, as compared to the lack of trend shown in Figure 8a. However, the data shown in Figure 8a are only from observations associated with Level 2 almucantar retrievals that have the additional more rigorous application of cloud screening of sky radiance data symmetry and effective sky radiance noise filtering. The result is only 6 days of data with Level 2 almucantars from November in the entire Mongu data set (see Figure 5 legend), while there are 223 days with level 2

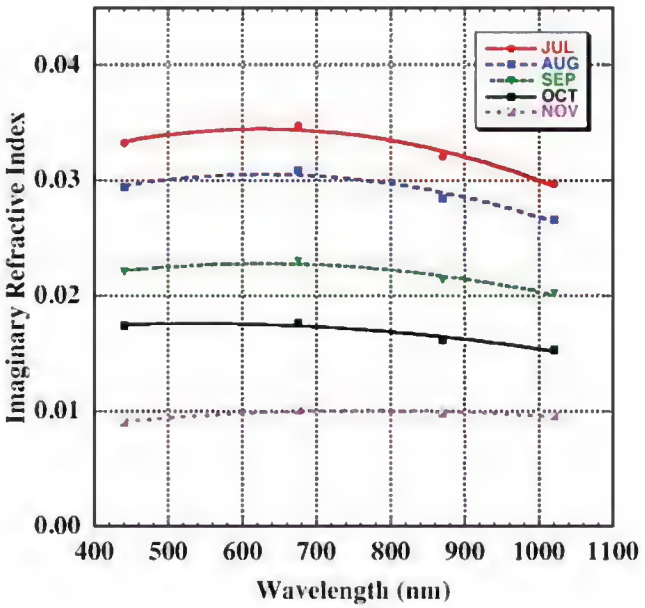

Figure 7. Monthly mean spectral imaginary refractive indices (similar to SSA in Figure 4) for the biomass-burning season months in Mongu, Zambia.

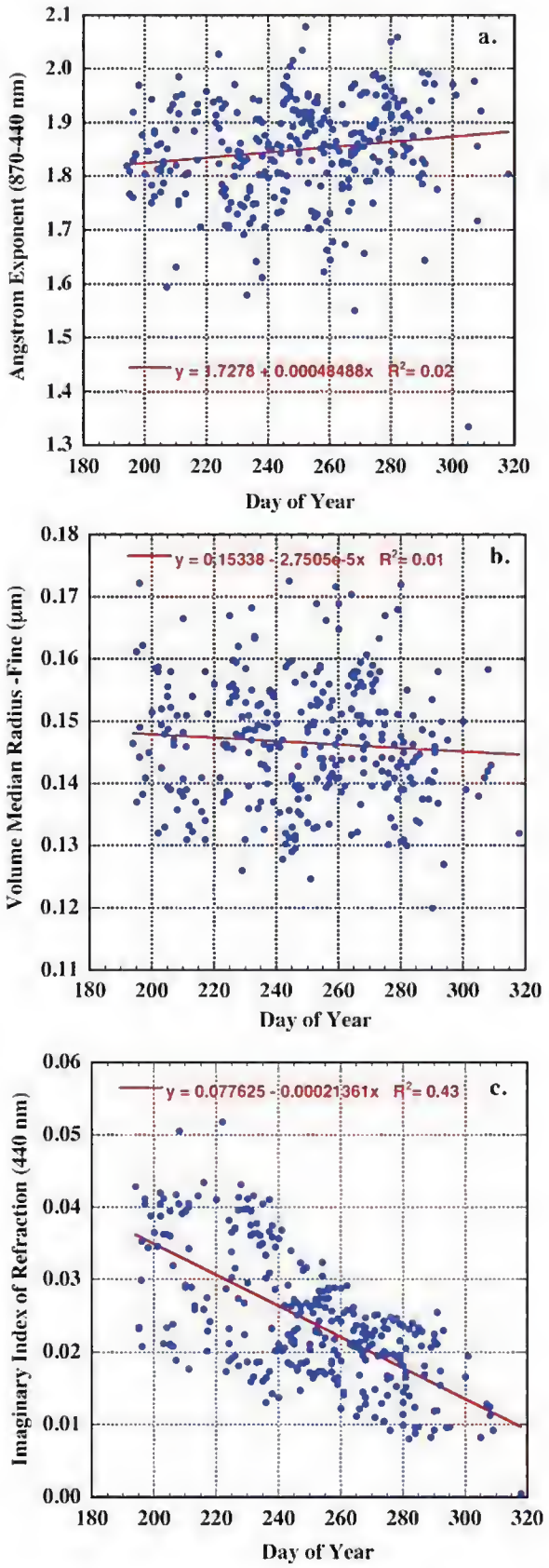

Figure 8. Time series at Mongu, Zambia during the biomass-burning season of daily means of (a) Ångström exponent (440–870 nm), (b) fine mode volume median radius (µm), and (c) 440 nm imaginary index of refraction.

direct sun AOD data shown in Figure 2, which include some days with partial cloud contamination.

[21] Prior studies have analyzed the AERONET volume size distribution retrievals in Mongu and other sites in Zambia [*Eck et al.*, 2001; *Dubovik et al.*, 2002; *Eck et al.*, 2003]. As previously mentioned, the mean volume radius for biomass-burning aerosols in this region from AERONET has compared well with in situ measurements, within ~0.005 µm radius [*Reid et al.*, 2005a]. In Figure 8b, the time series of fine-mode volume median radius from the AERONET retrievals shows most data within ~0.13 to 0.16 µm radius (mean = 0.146 µm), and with no seasonal trend ($r^2 = 0.01$), which is consistent with the lack of trend in Ångström exponent. Since aerosol size showed no trend throughout the burning season, this suggests that aerosol growth through aging, coagulation, or hygroscopic swelling (at higher relative humidity) can be ruled out as a significant underlying reason for the seasonal trend in single scattering albedo. The seasonal trend of the asymmetry parameter was also analyzed, and the percentage of variance explained by linear regression ranged from less than 0.1% to 1.5% from 440 nm to 870 nm. Therefore there was no significant observed trend in the AERONET retrievals of the aerosol scattering phase function throughout the biomass-burning season. The retrieved real part of the refractive index also shows no significant seasonal variation ($r^2 = 0.06$) and has a seasonal mean ranging from 1.49 at 440 nm to 1.51 at 1020 nm, therefore has little influence on the SSA trend. On the other hand, the imaginary index of refraction (Figure 8c), which accounts for absorption, does exhibit a significant downward seasonal trend. In fact, the linear regression fit explains 43% of the variance, very similar to the 49% of the variance explained by the SSA versus day of year linear fit seen in Figure 3b. Since we had previously suggested from analysis of the AAE that black carbon is likely the primary absorbing aerosol component at Mongu, then the downward trend in k suggests that the black carbon content in the aerosol is decreasing as the burning season progresses and is also the primary reason for the seasonal trend in SSA.

[22] In order to investigate whether this trend in SSA is a local phenomenon, we analyzed the data from the Etosha Pan, Namibia site which is ~885 km to the southwest of Mongu. The AERONET data from the Etosha Pan site were only available for one burning season, August to November 2000 for the SAFARI 2000 campaign. Hence, we analyzed individual almucantar retrievals versus day of year, rather than daily averages of the retrievals as was done previously for Mongu. Figure 9a shows the temporal trend of SSA, which is very similar to the trend observed at Mongu, in fact within less than 0.01 of the trends observed at Mongu for the years 2001 to 2004 (Figure 4) and with a similar r^2 value (0.69) from linear regression. The trend of decreasing imaginary refractive index as the burning season progresses (Figure 8b) at Etosha Pan is also very similar to the trend observed at Mongu, and the 69% of variance explained by the linear fit is the same as for the SSA trend at Etosha Pan. Similar to Mongu, there was no significant trend in aerosol size with Ångström exponent (440–870 nm) varying from ~1.5 to 2.1 indicating all fine mode dominated smoke, except for the two last points at day 318 that was a dust event with $a_{440\ 870} < 0.15$. Therefore, the similarity of the SSA and

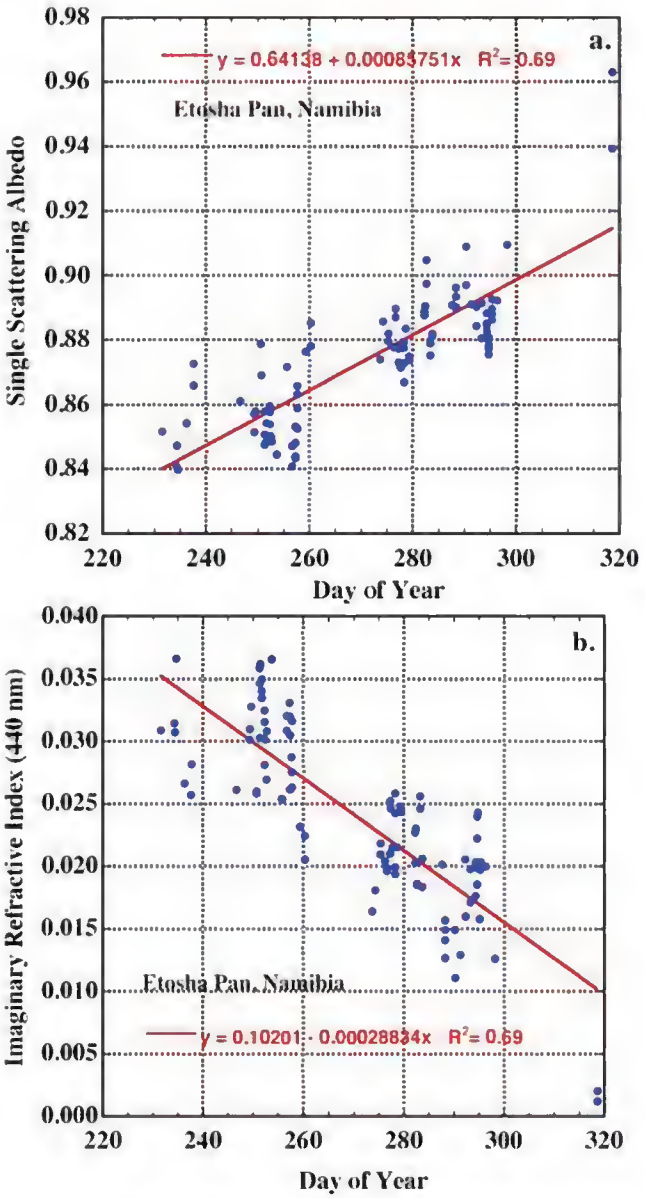

Figure 9. Biomass-burning season time series of individual retrievals at Etosha Pan, Namibia, for (a) single scattering albedo at 440 nm and (b) imaginary refractive index at 440 nm.

imaginary index trends at both Etosha Pan and Mongu suggests that this burning season trend in aerosol absorption is coherent over a relatively large region.

[23] The Skukuza, South Africa site is further yet from Mongu and in another direction, ~1395 km to the southeast. The SSA at 440 nm is plotted versus day of the year for this site in Figure 10. The seasonal trend in SSA at Skukuza shows mainly lower values in the primary biomass-burning season of July–October with large variation however versus higher values in other months. A significantly less coherent trend is seen throughout the burning season however than was observed at either the Mongu or Etosha Pan sites. There is no trend in Ångström exponent (440–870 nm) for the July–December interval (r^2 = 0.00; mean $a_{440\ 870}$ = 1.66), and while there is a downward trend in imaginary refractive index, it shows more scatter (r^2 = 0.10) than the trend in SSA (r^2 = 0.16) over the July–December interval. This variability may largely be due to mixtures of other aerosol types besides those from open biomass burning in this region. *Piketh et al.* [1999] analyzed in situ ground-based measurements at several sites in South Africa (including one very near Skukuza) and concluded that sulfate aerosol from industrial fossil fuel combustion and mineral dust was the main aerosol types in the region. Since sulfate is fine-mode nonabsorbing aerosol, the relatively high SSA values (and $a_{440\ 870}$ predominately higher than 1.40) retrieved by AERONET for the total atmospheric column at Skukuza were very likely the result of aerosol mixtures with a significant sulfate component.

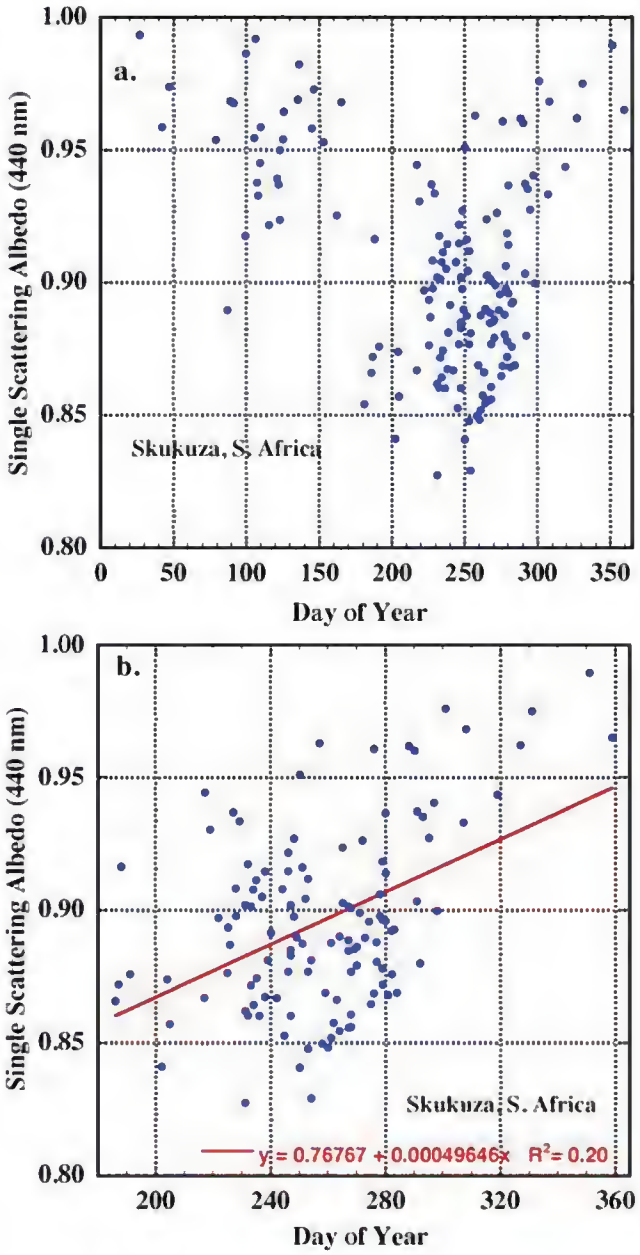

Figure 10. Time series of the SSA (440 nm) at Skukuza, South Africa, for (a) the entire year and (b) the biomass-burning season of July to December.

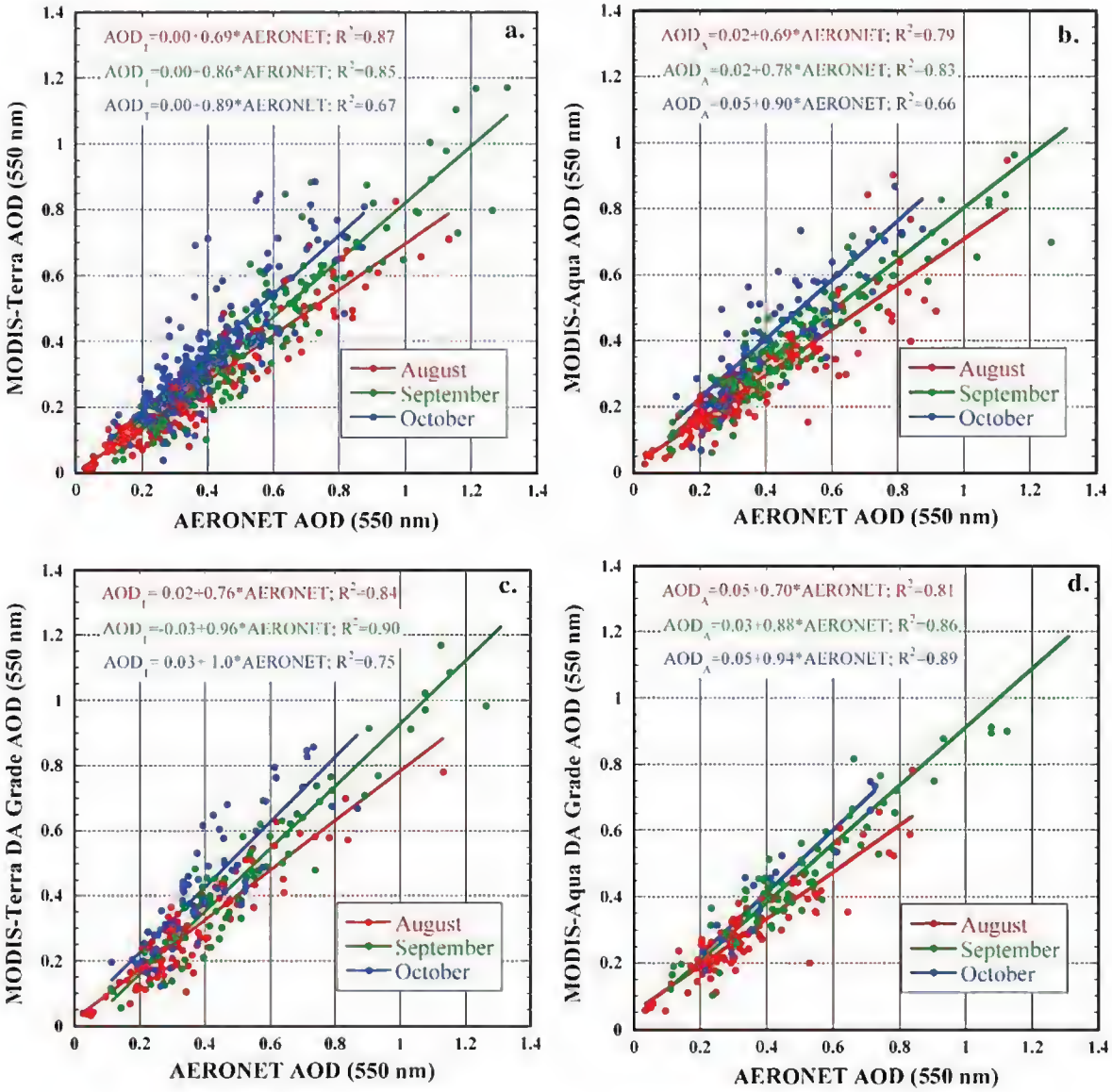

Figure 11. Comparison of MODIS retrievals (dark target algorithm) from both (a) Terra 2001–2010 and (b) Aqua 2003–2010 of AOD at 550 nm to AERONET measurements at Mongu, Zambia, with data separated for the primary burning season months of August, September, and October. Figures 11c and 11d are the same as Figures 11a and 11b but for the NRL data assimilation grade MODIS product of *Hyer et al.* [2011].

3.2. Seasonal Analysis of MODIS and MISR AOD Retrievals

[24] Any consistent seasonal shift in SSA has the potential to impact satellite AOD retrievals and thus result in a seasonally varying bias which could be perceived as random noise in a large verification study. Retrieval of AOD from the standard MODIS algorithms, for example, is dependent on the a priori assumption of a value of aerosol absorption [*Remer et al.*, 2005; *Levy et al.*, 2007a, 2007b]. Deviation from the assumed values has a compounding effect on retrieval bias as AODs increase into multiple scattering environments. AERONET measured AOD is highly accurate (~0.01 in the visible and near infrared) and therefore comparison to satellite retrievals allows for analysis of the likely reasons for potential biases, primarily either from errors in characterizing surface reflectance or in allowing for a realistic enough aerosol model. Given the high AODs found in the southern Africa smoke plume, the seasonal variation in AERONET inverted SSA provides a natural laboratory to test the impact of SSA on satellite AOD retrieval error. Indeed, as we found no systematic seasonal microphysical changes in the retrievals other than absorption, the Mongu site allows the examination of a rarely occurring "partial derivative" of satellite retrieval microphysical models.

[25] To begin, comparisons of AOD retrievals from both Terra and Aqua satellite MODIS sensors against the Mongu AERONET site are presented in Figures 11a and 11b, respectively. Comparisons of AOD are shown for 550 nm with the AERONET data being interpolated to 550 nm. This matchup was described in section 2. To observe the influence of seasonal variation of SSA, data are divided into the three core months of burning, August, September, and October,